

Accepted Manuscript

Is realistic Antarctic sea ice extent in climate models the result of excessive ice drift?

P. Uotila, P.R. Holland, T. Vihma, S.J. Marsland, N. Kimura

PII: S1463-5003(14)00052-3

DOI: <http://dx.doi.org/10.1016/j.ocemod.2014.04.004>

Reference: OCEMOD 892

To appear in: *Ocean Modelling*

Received Date: 28 October 2013

Revised Date: 10 April 2014

Accepted Date: 21 April 2014



Please cite this article as: Uotila, P., Holland, P.R., Vihma, T., Marsland, S.J., Kimura, N., Is realistic Antarctic sea ice extent in climate models the result of excessive ice drift?, *Ocean Modelling* (2014), doi: <http://dx.doi.org/10.1016/j.ocemod.2014.04.004>

This is a PDF file of an unedited manuscript that has been accepted for publication. As a service to our customers we are providing this early version of the manuscript. The manuscript will undergo copyediting, typesetting, and review of the resulting proof before it is published in its final form. Please note that during the production process errors may be discovered which could affect the content, and all legal disclaimers that apply to the journal pertain.

Is realistic Antarctic sea ice extent in climate models the result of excessive ice drift?

P. Uotila^{a,b}, P.R. Holland^c, T. Vihma^b, S.J. Marsland^a, N. Kimura^d

^a*CSIRO–Marine & Atmospheric Research, Aspendale, Australia*

^b*Finnish Meteorological Institute, Helsinki, Finland*

^c*British Antarctic Survey, Cambridge, the UK*

^d*National Institute of Polar Research, Tachikawa, Japan*

Abstract

For the first time, we compute the sea-ice concentration budget of a fully coupled climate model, the Australian ACCESS model, in order to assess its realism in simulating the autumn–winter evolution of Antarctic sea-ice. The sea-ice concentration budget consists of the local change, advection and divergence, and the residual component which represents the net effect of thermodynamics and ridging. Although the model simulates the evolution of sea-ice area reasonably well, its sea-ice concentration budget significantly deviates from the observed one. The modelled sea-ice budget components deviate from observed close to the Antarctic coast, where the modelled ice motion is more convergent, and near the ice edge, where the modelled ice is advected faster than observed due to inconsistencies between ice velocities. In the central ice pack the agreement between the model and observations is better. Based on this, we propose that efforts to simulate the observed Antarctic sea-ice trends should focus on improving the realism of modelled ice drift.

Keywords: thermodynamics, divergence, advection

*Corresponding author.

Email address: petteri.uotila@fmi.fi (P. Uotila)

1 1. Introduction

2 The Antarctic sea ice is expanding and climate models have difficulties
3 in simulating this trend (Turner et al., 2013a), for yet unknown reasons. A
4 small number of climate model simulations, however, show a similar increase of
5 Antarctic sea ice extent to the observed one which may indicate that the inter-
6 nal variability of the climate system, rather than forcing due to greenhouse gas
7 concentrations, plays a significant role (Zunz et al. , 2013). This hypothesis is
8 supported by Mahlstein et al. (2013), who studied Antarctic sea-ice area derived
9 from a large ensemble of 23 climate models and found that the internal sea-ice
10 variability is large in the Antarctic region indicating that both the observed and
11 modelled trends can represent natural variations along with external forcings.
12 Moreover, Polvani and Smith (2013) analysed forced and preindustrial control
13 model simulations of four climate models to see whether their Antarctic sea-ice
14 trends are due to the internal variability or not. They found that the observed
15 Antarctic trend falls within the distribution of trends arising naturally from
16 the coupled atmosphere–ocean–sea ice system and concluded that it is difficult
17 to attribute the observed trends to anthropogenic forcings. Consistent with
18 Polvani and Smith (2013), Swart and Fyfe (2013) show that when accounting
19 for internal variability, an average multi-model sea-ice area trend is statistically
20 compatible with the observed trend.

21 However, the validity of the hypothesis that the Antarctic sea-ice increase
22 is due to the internal variability of the climate system remains uncertain be-
23 cause the models used to test the hypothesis show biases in the mean state and
24 regional patterns, and overestimate the interannual variance of sea-ice extent,
25 particularly in winter (Zunz et al. , 2013). To confirm the argument of natural
26 variability, a model would have to explain the observed sea-ice increase while si-
27 multaneously responding to anthropogenic forcings. Hence, it appears that the
28 models can not be used to test precisely whether the observed sea ice expansion
29 is due to the internal variability of the climate system or not.

30 In addition to the above mentioned model based studies, a recent observa-

31 tional study supports to some extent the argument of internal variability. Meier
32 et al. (2013) analysed satellite data and showed that the Antarctic sea-ice ex-
33 tent in 1964 was larger than anytime during 1979–2012. This is a robust result,
34 because within the wide range of uncertainty in the 1964 satellite estimate, the
35 1964 ice extent is higher than the monthly September average of any of the years
36 of the satellite record from 1979–2012 and remains on the highest end of the
37 estimates even when taking into consideration the variation within the month.
38 According to Meier et al. (2013), the ice cover may currently be recovering from
39 a relatively low level back to higher conditions seen in the 1960s. Hence, this
40 result suggests that the current 33 year increase in the sea-ice extent is due to
41 the long-term variability of the climate system. Whether this long-term vari-
42 ability is only due to the internal variability or due to the combined effects of
43 forcings and the internal variability remains unclear.

44 Observations can also be used to show that the Antarctic sea ice concentra-
45 tion trends are closely associated with trends in ice drift or with trends related
46 to thermodynamics (Holland and Kwok, 2012). The observed Antarctic sea-ice
47 drift trends can be explained by changes in local winds and the aspects of local
48 winds can be attributed to large-scale atmospheric circulation modes (Uotila et
49 al. , 2013b), which have experienced significant changes in the last thirty years
50 (Solomon et al., 2007; Turner et al., 2013b). Moreover, Holland and Kwok (2012)
51 show where the evolution of Antarctic sea ice is controlled either by thermo-
52 dynamic or dynamic processes during its autumnal expansion and in winter.
53 This is particularly valuable because the relatively weak overall Antarctic sea
54 ice trend consists of strong regional but opposing trends (Turner et al., 2009).
55 Holland and Kwok (2012) suggest that, by comparing their observational results
56 with similarly processed climate model output, one can diagnose faults in a cli-
57 mate model due to thermodynamic or dynamic processes when simulating the
58 Antarctic sea ice. This is the motivation of our study — to investigate whether
59 a fully coupled climate model produces realistic contributions from thermody-
60 namic and dynamic sea-ice evolution. In this way we should be able to address
61 which processes in the model are too poorly represented to realistically simulate

62 the currently observed sea-ice state, its variability and its trends. Results from
63 such an analysis have not yet been published.

64 Related to this, recent studies have shown that coupled ocean-ice models,
65 where atmospheric states are prescribed, can reproduce observed Antarctic sea-
66 ice trends under realistic atmospheric forcing and/or when they are constrained
67 with observations. Massonnet et al. (2013) assimilated sea ice concentration into
68 an ocean-ice model to generate Antarctic sea-ice volume time series from 1980-
69 2008. Additionally, Zhang (2013) shows by an ocean-ice model that intensifying
70 winds result in increase in sea ice speed, convergence and sea-ice deformation.
71 The sea-ice deformation increases the volume of thick ice in the ocean-ice model
72 along with a significant sea-ice concentration increase in the Southern Weddell
73 Sea. Importantly, Holland et al. (2014, submitted) show that a free-running
74 ocean-ice model forced by atmospheric re-analyses can reproduce Antarctic sea-
75 ice concentration and drift trends as observed. Hence, atmospheric states of a
76 fully coupled climate model seem crucial for the modelled sea-ice trends. Ac-
77 cordingly, an assessment of the thermodynamic and dynamic processes related
78 to the evolution of sea-ice concentration in a fully coupled climate model is an
79 important next step to understand why climate models have not been able to
80 simulate Antarctic sea ice realistically.

81 We hypothesise that climate models simulate the seasonal evolution of inte-
82 grated Antarctic sea-ice area, and integrated extent, reasonably well, even with
83 relatively unrealistic dynamic and thermodynamic components of the sea-ice
84 concentration budget, partly due to the balancing of biases of these compo-
85 nents. For example, during its autumnal expansion sea ice is advected over a
86 larger area when its speed is higher, but at the same time it melts more at
87 the northernmost ice edge where the ocean and atmosphere are warm and the
88 thermodynamics limits the dynamical expansion of sea ice. In order to produce
89 observed regional sea-ice concentration trends in decadal time scales, and the
90 overall sea-ice area or extent trends for the right reasons, and therefore with the
91 correct mass, energy and momentum fluxes, climate models need to simulate
92 regional dynamical and thermodynamical processes correctly.

93 To test the success of our hypothesis, we compare modelled dynamic and
 94 thermodynamic components of the Antarctic April–October sea-ice concentra-
 95 tion budget as derived from the output of a well performing state-of-the-science
 96 climate model with the observed budget of Holland and Kwok (2012). The ob-
 97 served sea-ice concentration budget data of Holland and Kwok (2012) is only
 98 available from April to October which limits our analysis to these months. We
 99 present the models, methods and data used for this analysis in the next section.
 100 In the Results and Discussion section, we compare modelled sea-ice concentra-
 101 tion budgets with observed ones and discuss how their differences affect the
 102 sea-ice evolution. Finally, in the last section we present the main conclusions of
 103 this study along with their implications.

104 2. Methods and data

Table 1: Model experiments used in this study.

Name	Years	Short description and reference.
<i>historical</i>	1850–2005	Historical simulations that use evolving forcing such as volcanoes, aerosols, greenhouse gas concentrations and land use changes (Taylor et al., 2012).
<i>rcp85</i>	2005–2100	A future projection simulation forced with specified concentrations (RCPs), consistent with a high emissions scenario (Taylor et al., 2012).
<i>CORE-II IAF</i>	1948–2007	The second phase of The Coordinated Ocean-ice Reference Experiments (COREs) that uses inter-annually varying prescribed atmospheric forcing (IAF) of Large and Yeager (2009) under the experimental protocols introduced in Danabasoglu et al. (2014).

105 We analyse data from four *historical* and one *rcp85* realisation simulated by
 106 the Australian Community Climate and Earth-System Simulator coupled model
 107 version 1.0 (ACCESS1.0) and 1.3 (ACCESS1.3) as submitted to the phase five
 108 of the Coupled Model Inter-comparison project (CMIP5) database (Table 1,
 109 Figure 1 and Dix et al., 2013). ACCESS1.0 and ACCESS1.3 differ in two
 110 important aspects: their sea-ice albedos are different and their atmospheric
 111 cloud microphysics schemes are different. Both these differences can be expected
 112 to affect the sea-ice performance. Therefore we wanted to see how much their

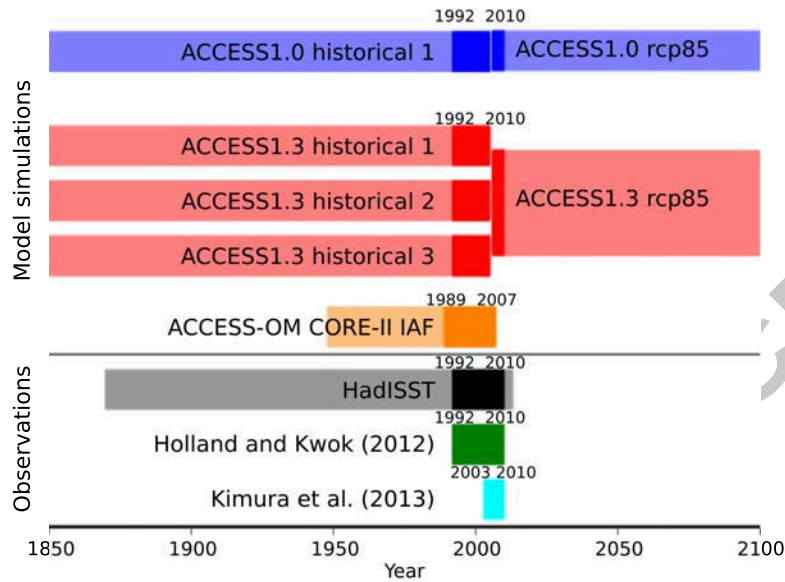


Figure 1: Horizontal bars illustrate total time extent of model simulations and observations used in this study. Time periods selected for the analysis are highlighted with non-transparent colours with the start and end years written, while time periods excluded from the analysis are shown with transparent, fainter colours.

113 sea-ice concentration budgets differ. The ACCESS configurations are one of
 114 the better performing CMIP5 models in terms of global sea-ice extent with a
 115 climatology relatively close to the observed one (Uotila et al., 2013a; Liu et al.,
 116 2013), thus justifying its selection for this study.

117 Moreover, similar analysis as for the ACCESS coupled model (ACCESS-
 118 CM; Bi et al., 2013a) output, are carried out for the output from an ACCESS
 119 ocean-sea ice model (ACCESS-OM; Bi et al., 2013b) simulation forced with
 120 prescribed atmospheric conditions and bulk formulae of Large and Yeager (2009)
 121 following the Coordinated Ocean-ice Reference Experiment phase 2 Inter-annual
 122 Forcing (CORE-II IAF) protocols as described in Griffies et al. (2012) (Table
 123 1). Following Danabasoglu et al. (2014), we use the fifth cycle of a CORE-II
 124 IAF simulation for the analysis of ACCESS-OM presented here. Note that the

125 ACCESS-OM simulation ends in 2007 which is the last year of CORE-II IAF.

126 The ACCESS-CM and ACCESS-OM configurations share the ocean and
127 sea-ice models and by analysing their differences we can assess the role of the
128 prescribed atmospheric forcing in driving changes in the Antarctic sea-ice con-
129 centration. The sea-ice model of ACCESS is the LANL Community Ice Code
130 version 4.1 Hunke and Lipscomb (2010), which uses the elastic-viscous-plastic
131 rheology, and the ocean model is an implementation of the 2009 public release
132 of the NOAA/GFDL MOM4p1 community code (Griffies et al., 2009). Both
133 ACCESS-CM and ACCESS-OM use an identical horizontal discretisation on an
134 orthogonal curvilinear tripolar grid with a nominal one degree resolution hav-
135 ing additional refinements in the Arctic, in the Southern Ocean, and near the
136 Equator. The ACCESS-CM atmospheric model has a horizontal resolution of
137 1.25° latitude by 1.875° longitude. ACCESS-OM is forced by CORE forcing
138 with spherical T62 resolution (approximately 1.9°), although many meteorolog-
139 ical variables, such as winds, are based on the NCEP/NCAR reanalysis with a
140 coarser horizontal resolution of 2.5° latitude \times 2.5° longitude.

141 There is a significant difference in the computation of sea-ice surface en-
142 ergy balance between ACCESS-CM and ACCESS-OM. As described in Bi et
143 al. (2013a) ACCESS-CM has a semi-implicit atmospheric boundary layer that
144 requires determination of the surface heat flux using a zero-layer thermody-
145 namic calculation following Semtner (1976). In contrast, ACCESS-OM uses a
146 4-layer sea-ice thermodynamic discretisation that allows for a more realistic in-
147 ternal sea-ice temperature profile. In the multi-layer thermodynamic approach
148 (ACCESS-OM), the sea-ice temperatures and net top and basal surface heat
149 fluxes are together calculated iteratively, with a heat capacity that depends on
150 internal material properties. The simpler zero-layer approach (ACCESS-CM)
151 only accounts for top and basal sea-ice temperatures and assumes a linear in-
152 ternal sea-ice temperature profile with no heat capacity. As shown by Cheng
153 et al. (2008), an increased number of sea ice layers results in more realistic sea-
154 ice thermodynamics. Despite this difference, having both ACCESS-CM CMIP5
155 and ACCESS-OM CORE-II simulations available is clearly an asset for our

156 evaluation that is not available for many climate models.

Following Holland and Kwok (2012), we compute April–October (from 1 April to 31 October) daily sea-ice concentration budgets for ACCESS-CM realisations and for the ACCESS-OM experiment as,

$$\frac{\partial A}{\partial t} + \mathbf{u} \cdot \nabla A + A \nabla \cdot \mathbf{u} = f - r, \quad (1)$$

157 based on daily sea-ice concentration (A) and velocity (\mathbf{u}). The concentration
158 change from freezing minus melting (f), and the concentration change from
159 mechanical ice redistribution processes (r), such as ridging and rafting, are
160 resolved as a residual component ($f - r$). In general, and in the Antarctic in
161 particular, where the sea-ice drift tends to be divergent, the magnitude of f can
162 be expected to be much larger than that of r .

Next, daily sea-ice concentration budgets are integrated over the April–October period for each year. The integral of the first term from the left in (1) provides the net change in the sea-ice concentration from the beginning to end of the period. The integral of the second term in (1) is the contribution to the sea-ice concentration change by the advection, the integral of the third term is the contribution by the divergence and the integral on the right hand side is the net contribution by the thermodynamic and ridging processes. After reorganising, the integrated ice concentration budget can be represented as,

$$\int_{t_1}^{t_2} \frac{\partial A}{\partial t} dt = - \int_{t_1}^{t_2} \mathbf{u} \cdot \nabla A dt - \int_{t_1}^{t_2} A \nabla \cdot \mathbf{u} dt + \int_{t_1}^{t_2} (f - r) dt, \quad (2)$$

where we denote the term on the left hand side of (2) as difference or *dadt*; the first term on the right hand side as advection or *adv*; the second term as divergence or *div*; and the third term as residual or *res*. Accordingly, the integrated budget and its components can be expressed compactly as

$$dadt = adv + div + res. \quad (3)$$

163 It is important to understand that the three components on the right hand
164 side of (3) are interdependent and, for example, regions experiencing large rates
165 of divergence are likely to experience ice growth under cold atmospheric condi-
166 tions. Another example would be a case where the ice melt decreases the sea-ice
167 concentration and thickness, and consequently results in a faster moving sea ice,
168 which in turn affects the divergence and advection.

169 Finally, integrated components of sea-ice concentration budget are used to
170 compute their average values over 19-year periods of 1992–2010 (ACCESS-CM)
171 and 1989–2007 (ACCESS-OM). These periods were selected because they are
172 as close as possible to the observational results covering 1992–2010, which is the
173 longest period with reliable sea-ice concentration budget observations available
174 (Holland and Kwok, 2012). The observed sea-ice concentration budget was cal-
175 culated on a 100×100 km² grid, which has a resolution close to the ACCESS
176 model grid (nominally 1° latitude \times 1° longitude). Following Holland and Kwok
177 (2012), we apply a low pass filter, where every grid point is replaced by the
178 mean value of a 9-cell square centred on that point, on *adv*, *div*, and *res* in (3)
179 to ensure the comparability of the model output with the observations. Model
180 based results are robust and rather similar with or without the smoothing, but
181 Holland and Kwok (2012) observation based results require smoothing to re-
182 duce grid-scale noise in the derivatives. Note that to cover the whole 1992–2010
183 period we joined four ACCESS-CM *historical* simulations, which end in 2005,
184 with the *rcp85* simulation from 2006–2010 resulting in four combinations of time
185 series – one combination for ACCESS1.0 and three for ACCESS1.3 (Figure 1).
186 To quantify the similarity between the observed and modelled sea-ice, the nor-
187 malised root-mean-square-error (NRMSE) was computed between the observed
188 and modelled sea-ice concentration. We also compare the modelled sea-ice area,
189 computed as the area integral of ice concentration, with the sea-ice area based
190 on observational HadISST data (Rayner et al., 2003), and we assess the agree-
191 ment of modelled ice drift with a 2003–2010 ice velocity climatology computed
192 from observation based data (Kimura et al., 2013). Kimura et al. (2013) have re-
193 cently published a daily ice velocity product on a 37.5 km resolution grid which

194 is prepared using the satellite passive microwave sensor Advanced Microwave
 195 Scanning Radiometer for EOS (AMSR-E) data over years 2003–2011.

196 3. Results and discussion

197 3.1. General characteristics

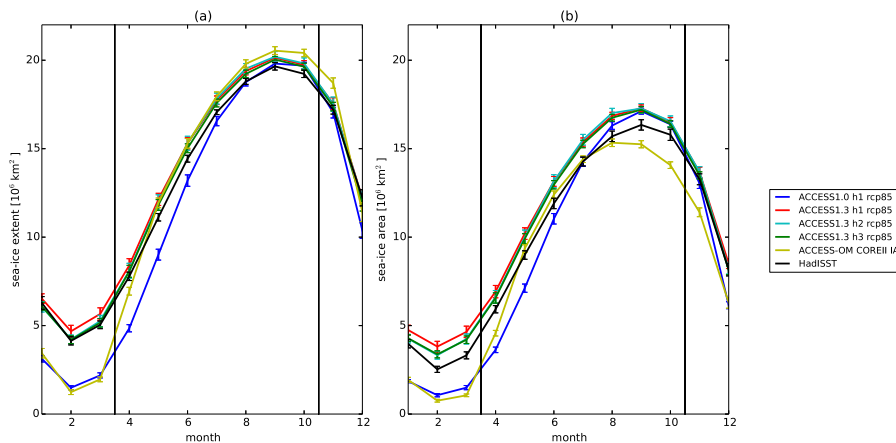


Figure 2: Monthly mean sea-ice (a) extent and (b) area climatologies derived from observational HadISST data and ACCESS model output. HadISST and ACCESS-CM climatologies are based on 1992–2010 time period, while the ACCESS-OM climatology is based on 1989–2007 time period. Vertical bars indicate 95% confidence limits of monthly means. The beginning of April and the end of October are marked with black vertical lines. Sea-ice extent is the integral of grid cells areas where the sea-ice concentration is larger than 15%, while sea-ice area is the area integral of ice concentration.

198 Monthly climatologies of Antarctic sea-ice extent, area and concentration
 199 derived from ACCESS simulations and the HadISST observational product are
 200 presented in Figures 2 and 3. The sea-ice extent is defined as the integral of
 201 grid cells areas where the sea-ice concentration is larger than 15%. The sea-ice
 202 area is computed as the integral of grid cells areas multiplied by the sea-ice
 203 concentration in each grid cell. ACCESS-OM and ACCESS1.0 simulations have
 204 lower than observed April sea-ice extents, areas and concentrations in contrast
 205 to ACCESS1.3 April sea-ice extents, areas and concentrations which are close
 206 to and higher than observed, respectively. In October, ACCESS-CM sea-ice

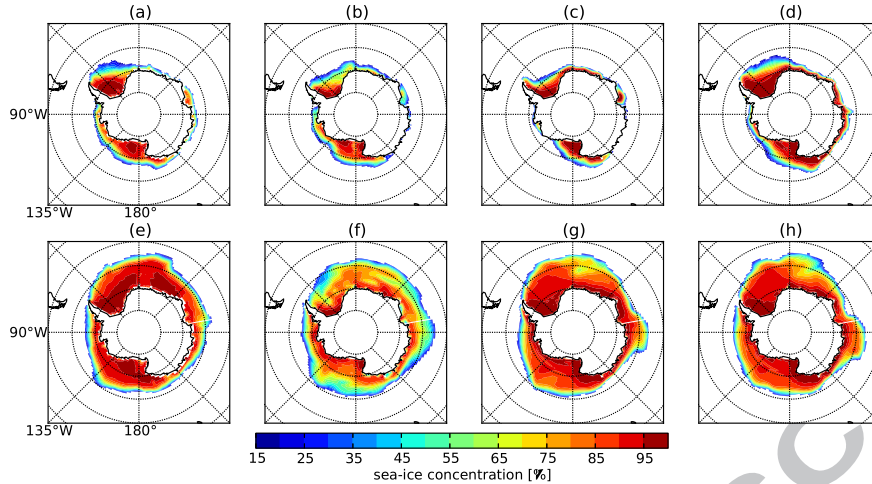


Figure 3: April (a-d) and October (e-h) mean sea-ice concentration for (a,e) HadISST from 1992–2010, (b,f) ACCESS-OM from 1989–2007, (c,g) ACCESS1.0 ensemble from 1992–2010 and (d,h) ACCESS1.3 ensemble from 1992–2010.

207 extents and areas are slightly higher than observed (Figure 2) while ACCESS-
 208 CM sea-ice concentrations are lower than observed in the Weddell Sea and in
 209 the Ross Sea (Figure 3). The ACCESS-OM sea-ice extent (area), however, is
 210 significantly higher (lower) than observed in October (Figure 2). As shown in
 211 Figure 3f, the ACCESS-OM sea-ice concentration is low everywhere resulting in
 212 the too low sea-ice area, while the sea-ice extends too far off the coast of East
 213 Antarctica between 40°E and 110°E contributing to the too high sea-ice extent.
 214 Differences between October and April sea-ice areas are significantly larger in
 215 ACCESS1.0 simulations ($12.7\text{--}12.9 \times 10^6 \text{km}^2$) than observed ($9.9 \times 10^6 \text{km}^2$), and
 216 close to the observed in ACCESS1.3 and ACCESS-OM simulations, being 9.5--
 217 9.9 and $9.5 \times 10^6 \text{km}^2$, respectively.

218 The evolution of sea-ice extent and area from April to October varies consid-
 219 erably between ACCESS simulations. The April–August sea-ice extent and area
 220 increases in the ACCESS-OM simulation and particularly in the ACCESS1.0 ap-
 221 pear high, because their April sea-ice extents and areas are lower than observed
 222 and their August sea-ice extents and areas are close to or higher than observed
 223 (Figure 2). ACCESS1.3 simulations have close to the observed sea-ice area

224 increase from April to September and its sea-ice area remains higher than ob-
225 served. As a result, both ACCESS-CM model configurations produce too high
226 sea-ice area maxima in September although their sea-ice extents remain close
227 to the observed. This indicates that, on the average, the winter ACCESS-CM
228 sea-ice concentration is higher than observed. After September, the Antarctic
229 sea ice starts to retreat and ACCESS-CM sea-ice extents decrease at observed
230 rates, but ACCESS-CM sea-ice areas decrease at higher rates than observed
231 until October. This discrepancy is due to the thinner than observed ACCESS-
232 CM sea ice in the central ice pack, where the ice melt impacts the sea-ice area
233 rather than the sea-ice extent, and is manifested as a lower than observed sea-ice
234 concentration (Figure 3g and h). The faster than observed September–October
235 retreat indicate that the modelled sea ice responds to the atmospheric or oceanic
236 forcing too strongly during these months.

237 The ACCESS-OM sea-ice extent peaks in September, while its sea-ice area
238 peaks in August. This is due to the too thin ACCESS-OM sea ice in the
239 central ice pack, which starts melting in August while the sea-ice is still ex-
240 panding northwards driven by CORE-II IAF atmospheric states. Because the
241 average ACCESS-OM sea-ice concentration is lower than observed, the Sep-
242 tember ACCESS-OM sea-ice area is lower than observed even when its sea-ice
243 extent is higher than observed. To understand more in detail which processes
244 are driving the evolution of ACCESS sea ice, we next explore to which extent
245 the April–October evolution of sea ice is driven by its dynamical and thermo-
246 dynamical components.

247 Holland and Kwok (2012) computed the components of sea ice concentration
248 budget in wintertime (April–October) satellite data from 1992–2010 when the
249 Antarctic sea-ice cover experiences its seasonal northward expansion (Figures
250 2 and 4a). During the expansion, the sea-ice concentration increases from zero
251 to close to 100% in the ice pack around the continent, especially in longitudes
252 20°W–30°E in the Weddell Sea, as the ice edge advances northward (Figure
253 4a). The advection of sea ice contributes to the autumnal increase of sea-ice
254 concentration mainly along the northernmost perimeter of the maximum sea-

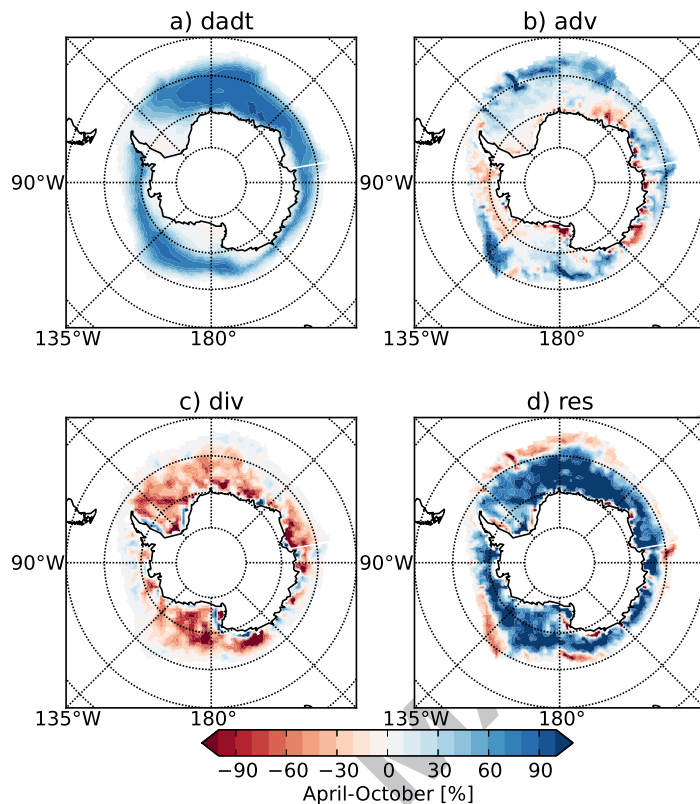


Figure 4: April–October 1992–2010 mean of each component in the ice concentration budget based on observational SSM/I data (Holland and Kwok, 2012).

255 ice area (Figure 4b). The divergent ice motion in the central ice pack decreases
 256 the ice concentration, which then, under low air temperatures, enhances the
 257 thermodynamic ice growth and increases the ice concentration (Figures 4c and
 258 d).

259 In some limited coastal regions, such as east of the Antarctic Peninsula and
 260 along the coast of the western Ross Sea, the ice converges and the residual
 261 component is negative (Figures 4c and d). It should be noted here that the
 262 Holland and Kwok (2012) observational sea-ice concentration budget does not
 263 allow us to consider these regions nearest to the coast where large rates of

264 divergence and freezing occur in autumn and winter. We can not calculate the
265 divergence ($\nabla \cdot \mathbf{u}$) there from the observational data, because the ice velocity
266 near the coastline has a significant sub-pixel geometry, so to call one pixel 'land'
267 and ascribe the zero flow there is potentially incorrect — hence $\nabla \cdot \mathbf{u}$ remains
268 unknown. Moreover, ∇ is highly uncertain since the coastline is poorly resolved.
269 However, we can calculate $\nabla \cdot \mathbf{u}$ over larger regions next to the coast, although
270 not at the pixel scale. Therefore the Holland and Kwok (2012) approach can
271 only really show the sea-ice divergence and the residual term on the large scale
272 and on finer scales in the inner pack away from the coast. The model output
273 doesn't have this issue, but regions at the immediate vicinity of the coast can
274 not be compared between model based and observation based results, and were
275 not included in the analysis.

276 Another region where the residual component is negative is at the north-
277 ern limit of Antarctic sea ice extent, where the ice melts after being advected
278 into these warm regions (Figures 4b and d). Hence, even though the residual
279 component is generally positive, indicating the dominance of thermodynamical
280 processes because ridging cannot create ice area, it can become negative under
281 certain circumstances — when the ice is compressed and ridging deformation oc-
282 curs, or when the ice melts. Overall, the observed sea-ice concentration budget
283 provides an insightful picture of the roles of the various physical processes con-
284 tributing to the autumn–winter evolution of Antarctic sea ice and is a valuable
285 diagnostic tool.

286 3.2. Simulations with prescribed atmosphere

287 Mean components of the ACCESS-OM CORE-II IAF sea-ice concentration
288 budget are shown in Figure 5. General features of April–October rate of sea-ice
289 concentration change agree with observations (compare Figure 5a with Figure
290 4a). The increase in sea-ice concentration occurs in the band extending from
291 the Weddell Sea around East Antarctica, the Ross Sea and the Amundsen Sea
292 to the Bellingshausen Sea. In the southern Weddell Sea and the southern Ross
293 Sea the ice concentration is similar in both the ACCESS-OM simulation and in

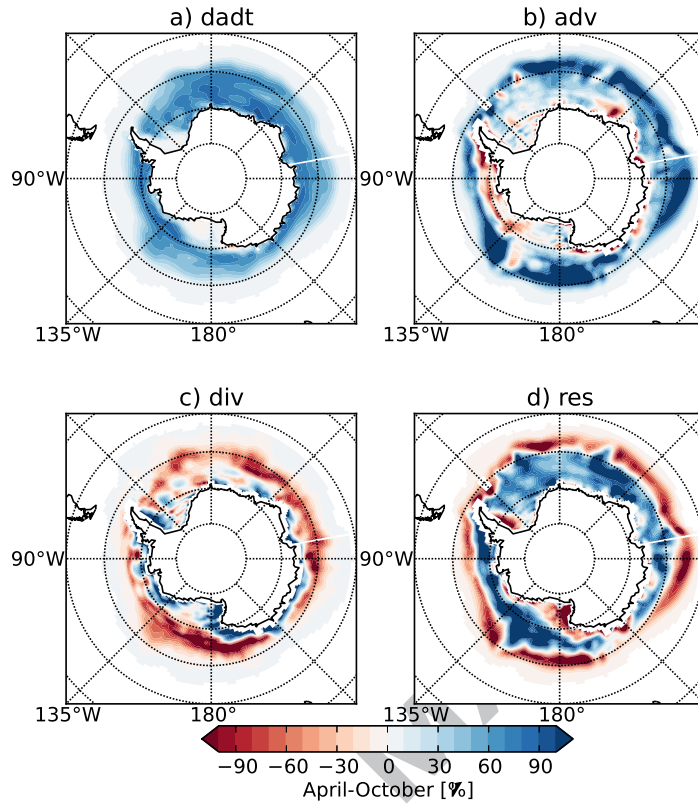


Figure 5: April–October 1989–2007 mean of each component in the ice concentration budget based on the ACCESS-OM CORE-II IAF simulation.

294 observations.

295 Despite similar general features between ACCESS-OM and observations,
 296 there are also significant differences, particularly in coastal regions, where the
 297 ACCESS-OM sea-ice concentration increases more than observed due to the fact
 298 that at the beginning of April the ACCESS-OM ice area is lower than observed
 299 (Figure 2). This results in a broader than observed band of sea ice concentra-
 300 tion increase (Figure 5a). On the contrary, the ACCESS-OM ice concentration
 301 increases less than observed in the Weddell Sea and in the Pacific Sector, from
 302 170°E to 90°W, which is the reason why the September ACCESS-OM sea-ice
 303 area remains lower than observed (Figure 2).

304 The ACCESS-OM and observations disagree at the northernmost edge of
305 the sea ice. The ACCESS-OM April–October ice concentration change is higher
306 than observed around East Antarctica where the ice is advected too far north
307 (Figures 4b and 5b). In the northern Weddell Sea, the ACCESS-OM residual
308 term is too small due to a combination of strong advection and weak divergence
309 (Figures 4 and 5), and results in a negative bias in the ACCESS-OM April–
310 October ice concentration change. Hence, although some general features of
311 ACCESS-OM ice advection match with observations — the ice is transported
312 from the coastal regions, where the advection decreases the ice concentration,
313 to the north where the ice concentration increases (Figures 4b and 5b) — the
314 ACCESS-OM ice advection results in positive ice concentration biases close
315 to the edge of the maximum ice extent, which are indicated in the residual
316 component as excessive melting (Figure 5d). We further note that the large
317 north-south gradients in the residual term partly originate from the fact that
318 the mean for April–October is only calculated on the basis of the sub-period
319 when there is sea ice in a certain region; the northernmost regions are not
320 affected by the autumn freezing.

321 In the central ice pack and close to the coast, the ACCESS-OM sea-ice
322 divergence values are largely offset by values of the residual component (Figures
323 5c and d). In coastal regions, the convergent ice motion positively contributes to
324 ice concentration, but away from the coast the opposite occurs as the divergent
325 ice motion decreases the ice concentration. As seen in Figure 4c, the Antarctic
326 ice motion is mainly divergent and the (coastal) area of convergent motion is
327 very small according to observations. In the ACCESS-OM simulation, however,
328 the area of convergent motion is much larger and correspondingly the observed
329 area of divergent motion is much smaller (Figure 5c). This is associated with the
330 fact that the ACCESS-OM residual component is quite different than observed,
331 as seen from Figure 5d, where the blue area, signifying the thermodynamic
332 growth of ice, is much smaller than observed (Figure 4d). Accordingly, two and
333 very likely interdependent biases are obvious: the ACCESS-OM coastal ice drift
334 is too convergent; and the areas of thermodynamic growth are too limited and

335 near the coast overtaken by the mechanical deformation.

336 Although the April–October ice concentration change appears similar in
337 ACCESS-OM and in observations, contributions by the advection, the diver-
338 gence and the residual component are notably different. A significant part of
339 the difference between ACCESS-OM and observations is due to the ice motion,
340 namely the extensive convergence near the coast and too strong advection off
341 the coast in ACCESS-OM. This is due to too high ACCESS-OM ice velocities,
342 as we show at the end of this section. The simulation of sea ice in the Southern
343 Ocean is sensitive to wind forcing and its resolution especially along the Antarc-
344 tic coast (Stössel et al., 2011). Because the surface wind is the most important
345 factor driving the ice drift, inaccuracies in the CORE-II IAF atmospheric states
346 are likely to deviate the modelled ice drift from observed and explain part of the
347 disagreement. The prescribed reanalysis atmospheric state tends to constrain
348 the modelled sea-ice extent to that observed because reanalysis atmospheric sur-
349 face variables are impacted by observed surface conditions including the sea-ice
350 concentration and the sea surface temperature.

351 It is important to note that biases in the divergence and in the residual
352 component largely balance each other resulting in a relatively realistic seasonal
353 evolution of sea-ice concentration which is driven by advection to a larger degree
354 than is observed. The lack of thermodynamic growth is more apparent in the
355 ice thickness than ice concentration and the ACCESS-OM ice remains too thin
356 partly because the ice velocity is excessively fast, and the ice thus advances north
357 too early and partly because of a warm and overly convective Southern Ocean
358 which is typical for the ACCESS model and for other ocean–ice models (Bi et
359 al., 2013b; Griffies et al., 2009; Marsland et al., 2003). Model parameterisations
360 also play an important part and can be used, for example, to adjust the sea-
361 ice evolution via heat conductivity, the air-ice momentum drag coefficient, the
362 ice-ocean stress turning angle and the mechanical deformation rates (Uotila
363 et al., 2012). In this paper we have found evidence that it is not enough to
364 adjust the model by selecting a set of parameter values that reproduce a realistic
365 looking ice concentration distribution, or area or extent, but the best set of

366 model parameters should produce as realistic looking components of sea-ice
 367 concentration budget as possible. Therefore we emphasise the importance of
 368 model velocity assessment against those observed.

Table 2: Area integrals of Antarctic April–October ice concentration budget mean components in 10^6 km² and in parenthesis as percentages of *dadt*. For ACCESS1.0 and ACCESS1.3 ensemble minimum and maximum values are listed.

Name	dadt	adv	(%)	div	(%)	res	(%)
Holland and Kwok (2012)	9.4	3.3	(35)	-5.0	(-53)	11.1	(118)
ACCESS-OM	11.0	10.8	(98)	-3.0	(-27)	3.2	(29)
ACCESS1.0	13.1–13.3	15.7–16.1	(121)	-6.5–-6.2	(-48)	3.6–3.7	(27)
ACCESS1.3	10.1–10.6	15.4–15.9	(151)	-9.1–-8.4	(-85)	3.3–3.5	(34)

369 Area integrals of sea-ice concentration budget components summarise how
 370 each component impacts the evolution of sea-ice area from April to October
 371 (Table 2). The ACCESS-OM April–October sea-ice area change is 1.6×10^6 km²
 372 larger than the observed mainly because the ACCESS-OM April sea-ice area is
 373 lower than observed (Figure 2). The ACCESS-OM ice advection is more than
 374 three times stronger than observed and is the dominant component in the sea-
 375 ice concentration budget. The ACCESS-OM ice is advected into regions where
 376 the prescribed CORE-II IAF near surface air temperatures are low enough that
 377 ice does not melt, but as the modelled advection is too strong, the ice advances
 378 north too soon and remains thin. The combined impact of divergence and resid-
 379 ual components in ACCESS-OM is much smaller than observed (0.2×10^6 km²
 380 compared to 6.1×10^6 km²). The small difference between the divergence and
 381 residual component further highlights the fact that these two components coun-
 382 terbalance in ACCESS-OM, and as a result the ACCESS-OM April–October
 383 sea-ice area change is close to observed despite being dominated by advection.
 384 The thermodynamics of sea-ice melt and freeze determine in-situ production
 385 and destruction of sea ice while the dynamical processes of advection and diver-
 386 gence redistribute existing sea ice. The thermodynamic and dynamic processes
 387 are tightly coupled, so that the strong sea-ice advection biases identified in the
 388 ACCESS models also manifest as strong biases in the thermodynamic term.

389 The ACCESS model uses the elastic-viscous-plastic rheology which causes ice

390 to response more sensibly to the wind than the classical viscous-plastic rheology,
391 particularly when the ice concentration is higher than 0.9 (Massonnet et al.,
392 2011). In the Antarctic, the ice motion is generally divergent and the role of
393 rheology is smaller than in the Arctic, and, as Massonnet et al. (2011) conclude,
394 the model skill is not limited due to model physics, but due to other factors
395 such as model resolution and atmospheric forcing.

396 It is possible that the ACCESS-OM air-ice drag coefficient is too large un-
397 der stably stratified conditions (which prevail over sea ice). This is not due
398 to aerodynamic roughness length, which is as low as 0.005 m in ACCESS-OM,
399 but due to the fact that the model applies a function (Holtslag and de Bruin,
400 1988) that reduces the drag coefficient with stability much less than most other
401 experimental functions (Andreas, 1998). It is also possible that, due to the
402 prescribed atmospheric states that drive the ACCESS-OM sea ice, important
403 atmosphere-ocean feedback mechanisms that would modify the atmosphere and
404 further impact the sea-ice concentration budget in a fully coupled model, are
405 missing. Therefore we discuss next how sea-ice concentration budgets in fully
406 coupled ACCESS-CM simulations compare with the ACCESS-OM sea-ice con-
407 centration budget and with the observed budget.

408 *3.3. Coupled simulations*

409 Components of the ACCESS-CM April–October sea-ice area change are
410 shown in Table 2. The April–October sea-ice area change is larger than ob-
411 served in ACCESS-CM due to the slightly too high October sea-ice area, and
412 particularly in ACCESS1.0 due to its low April sea-ice area (Figure 2). As
413 with ACCESS-OM, the ice advection dominates the sea-ice area budget, al-
414 most five times larger than the observed. Contrary to the ACCESS-OM di-
415 vergence, the area integrals of ACCESS-CM divergence are more negative than
416 the area integral of the observed divergence. Hence, the ACCESS-CM ice drift
417 is more divergent and the relative importance of divergence is larger in the
418 ACCESS-CM sea ice concentration budget (from -85 to -48%, Table 2) than in
419 the ACCESS-OM sea ice concentration budget (-27%, Table 2). ACCESS-CM

420 residual components are much smaller than observed and, as with ACCESS-
 421 OM, are associated with the very large positive values of the ice advection in
 422 the sea-ice concentration budget. Hence, although the April–October sea-ice
 423 area change is relatively close to the observed in ACCESS-CM, its components
 424 are very different from observed.

Table 3: NRMSE between modelled April–October sea-ice concentration budget mean components and observed April–October 1992–2010 sea-ice concentration budget mean components of Holland and Kwok (2012). For ACCESS 1.0 and ACCESS1.3 ensemble minimum and maximum values are listed. All correlation coefficients have p-values less than 0.05.

	ACCESS-OM	ACCESS1.0	ACCESS1.3
<i>dadt</i>	0.21	0.29	0.20–0.22
<i>adv</i>	0.08	0.11	0.10–0.11
<i>div</i>	0.11	0.10	0.11
<i>res</i>	0.11	0.13	0.13

425 How well then do the modelled sea-ice concentration budget components
 426 agree with observed components and is the ACCESS-OM sea-ice concentration
 427 budget more realistic than the ACCESS-CM sea-ice concentration budget? We
 428 address these questions quantitatively by using the NRMSE metric. As seen
 429 in Table 3, metrics for *dadt*, *adv*, *div* and *res* are similar for ACCESS-CM
 430 and ACCESS-OM simulations. Additionally, within the ACCESS-CM ensemble
 431 biases and metrics vary very little (Tables 2 and 3) and the multi-layer sea-
 432 ice thermodynamics scheme of ACCESS-OM does not cause better NRMSE
 433 compared to ACCESS-CM. Therefore, ACCESS-OM and ACCESS-CM sea-ice
 434 concentration budgets appear equally unrealistic.

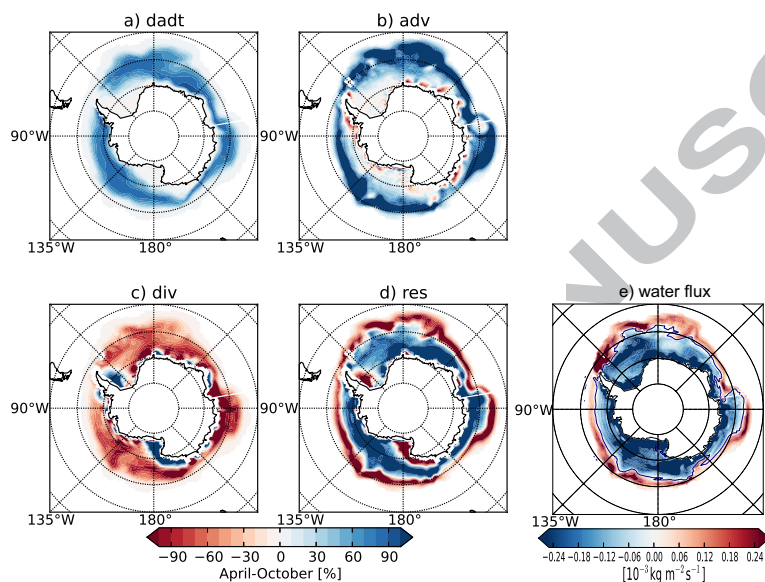


Figure 6: (a–d) April–October 1992–2010 mean of each component in the ice concentration budget based on the merged ACCESS1.3 historical ensemble member 1 and rcp85 simulations. (e) April–October 1992–2010 mean of the fresh water flux into the ocean due to freezing (negative flux) or melting (positive flux) of sea ice for the same simulations. This ensemble member rather than other members is plotted because it has the lowest NRMSE(*dadt*) with respect to the Holland and Kwok (2012) observations.

435 In addition to area integrals of sea-ice concentration budget components, it is
436 important to look at how sea-ice concentration budgets vary across the Antarc-
437 tic region in ACCESS-CM simulations. The ACCESS-CM sea-ice concentration
438 budget components based on the ensemble member that agrees best with ob-
439 servations according to Table 3 are shown in Figure 6. Although the general
440 advection pattern looks reasonable in the ACCESS-CM simulation, as was the
441 case for ACCESS-OM, the ice is advected along the boundary of the maximum
442 ice extent at much higher rates than observed (compare Figures 6b and 4b).
443 Regarding the ACCESS-CM divergence, the regions of convergence are not as
444 extensive as in the ACCESS-OM simulation, but still more widespread than in
445 observations (compare Figures 4c, 5c and 6c). Additionally, ACCESS-OM has
446 lower rates of sea-ice divergence and residual term in the central ice pack than
447 ACCESS-CM. However, the melting of sea ice along the boundary of the maxi-
448 mum sea-ice extent, which is larger than observed, reduces the area integral of
449 the ACCESS-CM residual component. Hence, the main reason for the disagree-
450 ment between the ACCESS-CM sea-ice concentration budget and the observed
451 sea-ice concentration budget is too strong ice advection in ACCESS-CM near
452 the ice edge, and the excessive convergence near the coast. A common factor of
453 these model–observation disagreements is the ice drift, which we analyse in the
454 next section.

455 Before analysing the ice drift we check how well the residual term corre-
456 sponds to the sea-ice thermodynamics. This is possible because the ACCESS-
457 CM simulation output includes the water flux into the ocean due to melting and
458 freezing of sea ice (Figure 6e). Although the water flux output is available as
459 monthly means and the residual term is based on daily data, the spatial agree-
460 ment between the ACCESS-CM residual (Figure 6d) and the water flux due to
461 thermodynamics is very good with regions of freezing (negative water fluxes)
462 matching the positive regions of the residual term in the central ice pack and
463 regions of melting matching the negative regions of the residual term close to
464 the ice edge. An exception is that in regions of convergent ice drift (western
465 Weddell Sea, southwestern Ross Sea, and a tongue further west of the latter;

466 Figure 6c), the residual term (Figure 6d) does not match with the fresh water
467 flux (Figure 6e). Please note here that the ice loss in the residual term near the
468 western sides of the Weddell and Ross seas is therefore from convergence and
469 ridging, which thickens the ice at the expense of ice area, as proposed by Hol-
470 land and Kwok (2012). Hence, our comparison supports the interpretation of
471 Holland and Kwok (2012) that the residual term provides a good representation
472 of the thermodynamic variability.

473 3.4. Ice drift

474 It has become apparent that the main reason for disagreement of ice concen-
475 tration budget between ACCESS and observations is the higher than observed
476 ice advection in ACCESS, and, as shown in equation (1), the main factor affect-
477 ing the ice advection is the drift speed. Consistent with the strong advection,
478 the mean April–October ice speed simulated by ACCESS is about two times
479 higher than the observational speed of Kimura et al. (2013). Hence, the reason
480 for the strong advection in ACCESS is the high drift speed.

481 Figure 7 highlights the regional differences between observations, ACCESS-
482 OM and ACCESS-CM. The coastal drift is too strong in ACCESS and while
483 impacting the advection it also generates the strong convergence zone where
484 the ice concentration increases (Figures 7, 5c and 6c). The extensive zone of
485 convergence could partly be a result of a relatively coarse ocean–ice model grid,
486 ranging from 0.25° at 78°S to 1° at 30°S , which does not resolve the coastal
487 velocities with the adequate accuracy. In addition, a high atmospheric resolution
488 is required to resolve winds which push newly formed sea ice away from the
489 coast. The CORE-II IAF winds are based on the NCEP/NCAR reanalysis and,
490 as shown by Stössel et al. (2011), an ocean–ice model forced with horizontal
491 resolution of 2.5° latitude \times 2.5° longitude NCEP/NCAR winds produces three
492 times less sea ice along the coast than the same model forced with $0.225^\circ \times$
493 0.225° high resolution winds. It is likely that even the $1.875^\circ \times 1.25^\circ$ horizontal
494 resolution of ACCESS-CM atmosphere is not high enough to resolve the coastal
495 wind field and increase the sea ice production.

496 In the central ice pack, such as in the central Weddell Sea, in the Ross Sea
497 and in the Amundsen–Bellingshausen Seas, the ACCESS ice speed is relatively
498 close to observed, but the direction of ACCESS ice velocity somewhat differs
499 from the observed velocities, particularly in the Weddell Sea where the ACCESS
500 ice velocity has a stronger westward component than observed (Figure 7). North
501 of the central ice pack, at the northernmost edge of the sea ice, the ACCESS
502 ice velocities are much higher than observed. It is certain that the regions of
503 higher-than-observed ice speed, close to the coast and at the ice edge, deviate
504 the ACCESS ice concentration budget from observed. These are, however, the
505 regions where the estimates of observed ice velocities are most uncertain which
506 increases uncertainties of the sea-ice concentration budget components.

507 It is clear that in Figure 5d and in 6d the ice growth is reasonable in the
508 pack (dark blue), so the low mean value of the residual term (Table 2) is coming
509 from the excessive red near the coast and at the ice edge. We have confirmed
510 that the negative residual near the coast is due to excessive ridging, which must
511 be from excessive velocity near the coast. It also seems highly likely that the
512 excessive melting near the ice edge is simply compensating excessive advection
513 into that region. In that sense the thermodynamics are wrong and they have
514 been adjusted to melt away the excessive ice flux towards the ice edge.

515 However, we still think the root cause of the problem is the dynamics. How
516 could excessive melting near the ice edge cause excessive advection (vdA/dy)
517 towards the ice edge? It is possible that an excessive dA/dy could contribute
518 but given that we have shown that v is far too large that seems like the obvious
519 culprit. Hence, it seems very likely that there is an excessive advection which
520 is bringing more ice into the melting zone and distorting the thermodynamics.

521 4. Conclusion

522 ACCESS models simulate the overall seasonal evolution of Antarctic sea-
523 ice extent and area realistically, but with contributions from the components
524 of the sea-ice concentration budget that significantly differ from contributions

525 based on observations of Holland and Kwok (2012). Accordingly, we accept
526 our research hypothesis that climate models simulate the seasonal evolution
527 of integrated Antarctic sea-ice area, and integrated extent, reasonably well,
528 even with relatively unrealistic dynamic and thermodynamic components of the
529 sea-ice concentration budget, mainly due to the balancing of biases of these
530 components. ACCESS models agree best with observations in the central ice
531 pack and disagree close to the Antarctic coast and at the ice edge. Because
532 these are the regions where the observation based estimates of ice drift are most
533 uncertain, it is reasonable to conclude that the true sea-ice concentration budget
534 is somewhere between model and observation based estimates.

535 The sea-ice concentration budget proved to be a valuable model diagnostic
536 tool for three reasons. First, the observation based estimates of Holland and
537 Kwok (2012) provide a very reasonable decomposition of the roles of the various
538 physical processes contributing to the autumn–winter evolution of Antarctic sea
539 ice and the integrated sea-ice area. Second, we showed that the sea-ice concen-
540 tration budget is sensitive to model configurations when we compared differences
541 between ACCESS-CM configurations and ACCESS-OM, and therefore it seems
542 that models can effectively be adjusted to reproduce the sea-ice concentration
543 budget components as realistically as possible. To further highlight this sen-
544 sitivity, we carried out an additional ACCESS-OM simulation (not described
545 above), otherwise identical to the one analysed in this study, but instead of
546 zero ice–ocean stress turning angle the simulation used a 16° ice–ocean stress
547 turning angle. As a consequence, the contribution of advection to sea-ice area
548 decreased to half and the contribution of the thermodynamics increased about
549 50%, but the contribution of divergence changed from negative to positive being
550 clearly unrealistic. Third, contributions of sea-ice concentration budget compo-
551 nents to the sea-ice area and regional evolution of sea ice are generally similar
552 in ACCESS-OM and ACCESS-CM. This indicates that, at least to some ex-
553 tent, the model adjustments required for the simulation of as realistic sea-ice
554 concentration budget components as possible can be carried out by using a
555 computationally cheaper ocean–sea ice model instead of a fully coupled model.

556 Specifically, our sea-ice concentration budget analysis revealed the strong
557 advection and the widespread coastal convergence in ACCESS due to the faster
558 than observed ice drift, which causes the simulated sea-ice concentration budget
559 to deviate from the observed. This erroneous balance of terms is important for
560 the oceanic processes — if the ice comes from advection rather than freezing,
561 then the sea-ice volume remains low and the ocean will feel only a fraction,
562 in our case one third, of the salt flux that it should receive. This reduced
563 salt flux might help to explain the oceanic warm bias in models, for instance.
564 Importantly, in order to reproduce the observed Antarctic sea-ice extent trend,
565 models have to be able to simulate the sea-ice concentration budget realistically
566 and therefore the ice drift and coastal convergence should be key focus areas of
567 model assessment and development.

568 **Acknowledgments.** This research was funded by the Academy of Finland
569 through the AMICO project (grant 263918) and by the Australian Govern-
570 ment Department of the Environment, the Bureau of Meteorology and CSIRO
571 through the Australian Climate Change Science Programme. This work was
572 supported by the NCI National Facility at the ANU. We thank the ACCESS
573 model development team for producing and making available their model out-
574 put.

575 Andreas, E. L. (1998) The atmospheric boundary layer over polar marine sur-
576 faces, In: Leppäranta, M. (Ed.), *Physics of Ice-Covered Seas*, Vol. 2., 715-773,
577 Helsinki University Printing House, Helsinki.

578 Bi, D., M. Dix, S. J. Marsland, S. O'Farrell, H. Rashid., P. Uotila, A. Hirst, E.
579 Kowalczyk, M. Colebiewski, A. Sullivan, Y. Hailin, N. Hannah, C. Franklin,
580 Z. Sun, P. Vohralik, I. Watterson, X. Zhou, R. Fiedler, M. Collier, Y. Ma,
581 J. Noonan, L. Stevens, P. Uhe, H. Zhu, R. Hill, C. Harris, S. Griffies, and
582 K. Puri (2013a) The ACCESS coupled model : Description , control climate
583 and evaluation, *Australian Meteorological and Oceanographic Journal*, 63(1),
584 41-64.

585 Bi, D., S. J. Marsland, P. Uotila, S. O'Farrell, R. Fiedler, A. Sullivan, S. M.

- 586 Griffies, X. Zhou, and A. C. Hirst (2013b) ACCESS-OM : the ocean and
587 sea-ice core of the ACCESS coupled model, *Australian Meteorological and*
588 *Oceanographic Journal*, 63(1), 213–232.
- 589 Cheng, B., Z. Zhang, T. Vihma, M. Johansson, L. Bian, Z. Li and H.
590 Wu (2008) Model experiments on snow and ice thermodynamics in the
591 Arctic Ocean with CHINARE2003 data, *J. Geophys. Res.*, 113, C09020,
592 doi:10.1029/2007JC004654.
- 593 Danabasoglu, G., S. G. Yeager, D. Bailey, E. Behrens, M. Bentsen, D. Bi, A.
594 Biastoch, C. Böning, A. Bozec, C. Cassou, E. Chassignet, S. Danilov, N.
595 Diansky, H. Drange, R. Farneti, E. Fernandez, P. G. Fogli, G. Forget, A.
596 Gusev, P. Heimbach, A. Howard, S. M. Griffies, M. Kelley, W. G. Large, A.
597 Leboissetier, J. Lu, E. Maisonnave, S. J. Marsland, S. Masina, A. Navarra, A.
598 J. George Nurser, D. S. y Mélia, B. L. Samuels, M. Scheinert, D. Sidorenko, L.
599 Terray, A.-M. Treguier, H. Tsujino, P. Uotila, S. Valcke, A. Voldoire, and Q.
600 Wang (2014) North Atlantic Simulations in Coordinated Ocean-ice Reference
601 Experiments phase II (CORE-II). Part I: Mean States, *Ocean Modelling*, 76–
602 107, doi:10.1016/j.ocemod.2013.10.005.
- 603 Dix, M., P. Vohralik, D. Bi, H. Rashid, S. J. Marsland, S. O’Farrell, P. Uotila, A.
604 C. Hirst, E. Kowalczyk, A. Sullivan, H. Yan, C. Franklin, Z. Sun, I. Watterson,
605 M. Collier, J. Noonan, L. Rotstayn, L. Stevens, P. Uhe, and K. Puri (2013)
606 The ACCESS Coupled Model Documentation of core CMIP5 simulations and
607 initial results, *Australian Meteorological and Oceanographic Journal*, 63(1),
608 83–99.
- 609 Griffies, S., A. Biastoch, C. Boning, F. Bryan, G. Danabasoglu, E. Chassignet,
610 M. England, R. Gerdes, H. Haak, R. Hallberg, W. Hazeleger, J. Jungclaus,
611 W.G. Large, G. Madec, A. Pirani, B.L. Samuels, M. Scheinert, A. Sen Gupta,
612 C.A. Severijns, H.L. Simmons, A.M. Treguier, M. Winton, M., S. Yeager, and
613 J. Yin (2009) Coordinated Ocean-ice Reference Experiments (COREs), *Ocean*
614 *Modelling*, 26(1-2), 1-46.

- 615 Griffies, S. M., Winton, M., Samuels, B., Danabasoglu, G., Yeager, S., Marsland,
616 S., Drange, H., and Bentsen, M. (2012) Datasets and protocol for the CLI-
617 VAR WGOMD Coordinated Ocean-sea ice Reference Experiments (COREs),
618 *WCRP Report No. 21/2012*, pp. 21.
- 619 Holland, P. R., and R. Kwok (2012) Wind-driven trends in Antarctic sea-ice
620 drift, *Nature Geoscience*, 5(11), 1–4, doi:10.1038/ngeo1627.
- 621 Holland, P. R., N. Bruneau, C. Enright, M. Losch, N. Kurtz, and R. Kwok
622 (2014) Modelled trends in Antarctic sea ice thickness, *J. Climate*, submitted.
- 623 Holtslag, A. A. M., and H. A. R. de Bruin (1988) Applied modeling of the
624 nighttime surface energy balance over land, *J. Appl. Meteorol.*, 37, 689-704.
- 625 Hunke, E.C. and Lipscomb, W.H. (2010) CICE: the Los Alamos Sea ice Model
626 Documentation and Software Users Manual. *LA-CC-06-012 Tech. Rep.*, 176.
- 627 Kimura, N., A. Nishimura, Y. Tanaka, and H. Yamaguchi (2013) Influence of
628 winter sea ice motion on summer ice cover in the Arctic, *Polar Res.*, Polar
629 Res., 32, 20193, doi:10.3402/polar.v32i0.20193.
- 630 Large, W. G., and S. G. Yeager (2009) The Global Climatology of an
631 Interannually Varying Air-Sea Flux Data Set, *Clim. Dyn.*, 33, 341-364,
632 doi:10.1007/s00382-008-0441-3.
- 633 Liu, J., M. Song, R. M. Horton, and Y. Hu (2013) Reducing spread in cli-
634 mate model projections of a September ice-free Arctic, *Proc. Nat. Acad. Sci.*,
635 doi:10.1073/pnas.1219716110.
- 636 Mahlstein, I., P. R. Gent, and S. Solomon (2013) Historical Antarctic mean sea
637 ice area, sea ice trends, and winds in CMIP5 simulations, *J. Geophys. Res.:*
638 *Atmospheres*, 118, 1–6, doi:10.1002/jgrd.50443.
- 639 Marsland, S. J., H. Haak, J. H. Jungclaus, M. Latif, and F. Röske (2003)
640 The Max-Planck-Institute global ocean/sea ice model with orthogonal

- 641 curvilinear coordinates, *Ocean Modelling*, 5(2), 91–127, doi:10.1016/S1463-
642 5003(02)00015-X.
- 643 Massonnet, F., T. Fichefet, H. Goosse, M. Vancoppenolle, P. Mathiot, and C.
644 K. Beatty (2011), On the influence of model physics on simulations of Arctic
645 and Antarctic sea ice, *Cryosph.*, 5, 687699, doi:10.5194/tcd-5-1167-2011.
- 646 Massonnet, F., P. Mathiot, T. Fichefet, H. Goosse, C. König Beatty, M. Van-
647 coppenolle, and T. Lavergne (2013) A model reconstruction of the Antarctic
648 sea ice thickness and volume changes over 1980–2008 using data assimilation,
649 *Ocean Modelling*, 64, 6775, doi:10.1016/j.ocemod.2013.01.003.
- 650 Meier, W. N., D. Gallaher, and G. G. Campbell (2013) New estimates of Arctic
651 and Antarctic sea ice extent during September 1964 from recovered Nimbus I
652 satellite imagery, *The Cryosphere*, 7(2), 699–705, doi:10.5194/tc-7-699-2013.
- 653 Polvani, L. M., and K. L. Smith (2013) Can natural variability explain observed
654 Antarctic sea ice trends? New modeling evidence from CMIP5, *Geophys. Res.*
655 *Lett.*, doi:10.1002/grl.50578.
- 656 Rayner, N. A., Parker, D. E., Horton, E., Folland, C. K., Alexander, L. V.,
657 Rowell, D., Kent. E. and Kaplan, A. (2003) Global analyses of sea surface
658 temperature, sea ice, and night marine air temperature since the late nine-
659 teenth century, *J. Geophys. Res.*, 108(D14), 4407, doi:10.1029/2002JD002670.
- 660 Semtner, A.J., (1976) A model for the thermodynamic growth of sea ice in
661 numerical investigations of climate, *J. Phys. Oceanogr.*, 63, 79–389.
- 662 Solomon, S., D. Qin, M. Manning, Z. Chen, M. Marquis, K.B. Averyt, M.Tignor
663 and H.L. Miller (eds.) IPCC (2007) Summary for Policymakers. In: *Climate*
664 *Change 2007: The Physical Science Basis. Contribution of Working Group I*
665 *to the Fourth Assessment Report of the Intergovernmental Panel on Climate*
666 *Change*. Cambridge University Press, Cambridge, United Kingdom and New
667 York, NY, USA.

- 668 Stössel, A., Z. Zhang, and T. Vihma (2011) The effect of alternative real-time
669 wind forcing on Southern Ocean sea ice simulations, *J. Geophys. Res.*, 116,
670 C11021, doi:10.1029/2011JC007328.
- 671 Swart, N. C., and J. C. Fyfe (2013) The influence of recent Antarctic ice sheet
672 retreat on simulated sea ice area trends, *Geophys. Res. Lett.*, 40, 4328–4332,
673 doi:10.1002/grl.50820.
- 674 Taylor, K. E., R. J. Stouffer, and G. A. Meehl, (2012) An Overview of
675 CMIP5 and the Experiment Design. *Bull. Am. Met. Soc.*, 93, 485–498,
676 doi:10.1175/BAMS-D-11-00094.1
- 677 Turner, J., Comiso, J. C., Marshall, G.J., Lachlan-Cope, T.A., Bracegirdle,
678 T.J., Maksym, T., Meredith, M.P., Wang, Z. and Orr, A. (2009) Non-annular
679 atmospheric circulation change induced by stratospheric ozone depletion and
680 its role in the recent increase of Antarctic sea ice extent, *Geophys. Res. Lett.*,
681 36(8), 1–5, doi:10.1029/2009GL037524.
- 682 Turner, J., T. J. Bracegirdle, T. Phillips, G. J. Marshall, and J. S. Hosking
683 (2013a) An Initial Assessment of Antarctic Sea Ice Extent in the CMIP5
684 Models, *J. of Climate*, 26(5), 1473–1484, doi:10.1175/JCLI-D-12-00068.1.
- 685 Turner, J., T. Phillips, J. S. Hosking, G. J. Marshall, and A. Orr (2013b) The
686 Amundsen Sea low, *Int. J. Climatol.*, 33(7), 1818–1829, doi:10.1002/joc.3558.
- 687 Uotila, P., O’Farrell, S., Marsland, S. J. and Bi, D. (2012) A sea-ice sen-
688 sitivity study with a global ocean-ice model, *Ocean Modelling*, 51, 1-18,
689 doi:j.ocemod.2012.04.002.
- 690 Uotila, P., S. O’Farrell, S. J. Marsland, and D. Bi (2013a) The sea-ice perfor-
691 mance of the Australian climate models participating in the CMIP5, *Aus-
692 tralian Meteorological and Oceanographic Journal*, 61(1), 121–143.
- 693 Uotila, P., T. Vihma, and M. Tsukernik (2013b) Close interactions between the
694 Antarctic cyclone budget and large-scale atmospheric circulation, *Geophys.
695 Res. Lett.*, 40, 1–5, DOI:10.1002/grl.50560, in press.

696 Zhang, J., (2013) Modeling the impact of wind intensification on Antarctic sea
697 ice volume, *J. Climate*, doi:10.1175/JCLI-D-12-00139.1

698 Zunz, V., H. Goosse, and F. Massonnet (2013) How does internal variability in-
699 fluence the ability of CMIP5 models to reproduce the recent trend in Southern
700 Ocean sea ice extent?, *Cryosphere*, 7(2), 451–468, doi:10.5194/tc-7-451-2013.

ACCEPTED MANUSCRIPT

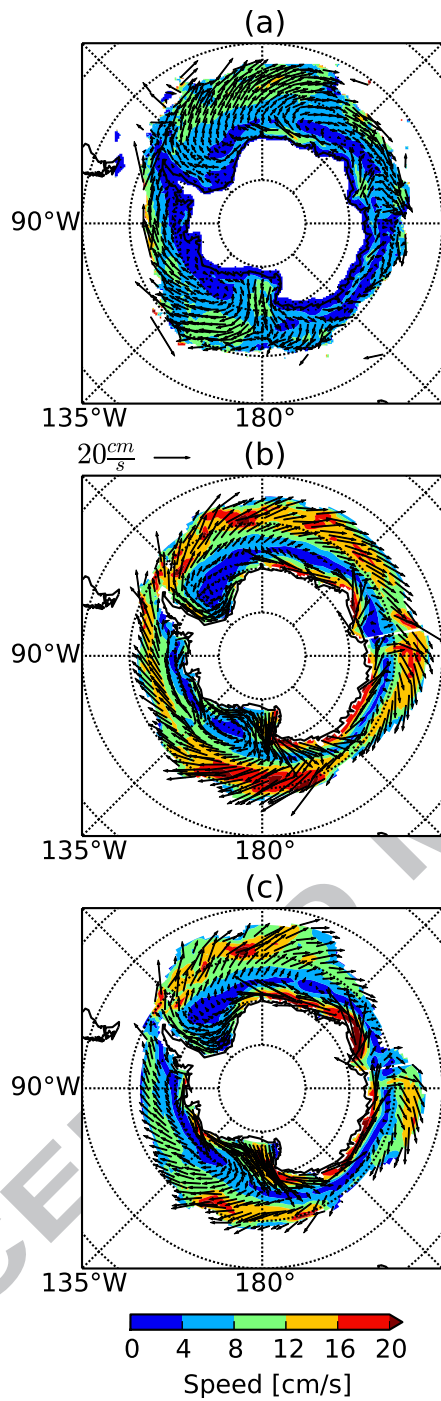


Figure 7: (a) 2003–2010 April–October mean ice velocity vectors and mean ice speed contour plot based on observational data of Kimura et al. (2013), (b) 1989–2007 ACCESS-OM CORE-II IAF April–October mean ice velocity vectors and speed, and (c) as (b), but based on the merged 1992–2010 ACCESS1.3 historical ensemble member 1 and rcp85 simulations.

Highlights:

- This is the first fully coupled climate model sea-ice concentration budget study.
- The modelled sea-ice concentration budget significantly deviates from the observed.
- The modelled ice motion is too convergent close to the coast.
- The modelled ice advection is too strong at the northmost ice edge.
- Model development should improve the realism of ice drift at these two regions.